Medium-resolution studies of extreme-ultraviolet emission from CO by electron impact

Isik Kanik, Geoffrey K. James, and Joseph M. Ajello

Jet Propulsion Laboratory, California Institute of Technology, Pasadena, California 91109

pp. 2067-2074

Medium-resolution studies of extreme-ultraviolet emission from CO by electron impact

Isik Kanik, Geoffrey K. James, and Joseph M. Ajello

Jet Propulsion Laboratory, California Institute of Technology, Pasadena, California 91109

We report medium-resolution [0.025 nm full width at half maximum (FWHM)] electron-impact-induced emission spectra of CO for 20-, 100-, and 200-eV impact energies. The emission spectra correspond to the extreme-ultraviolet transitions from the $B\,^1\Sigma^+(0)$, $C\,^1\Sigma^+(0)$, and $E\,^1\Pi(0)$ vibronic states to the $X\,^1\Sigma^+(0)$ ground state. The present measurements are carried out at 20 times higher spectral resolution (to separate the many blended components) compared to our previous measurements, which were at a spectral resolution of 0.5 nm FWHM. The emission cross sections corresponding to the $B\,^1\Sigma^+(0)$ $\rightarrow X\,^1\Sigma^+(0)$, $C\,^1\Sigma^+(0) \rightarrow X\,^1\Sigma^+(0)$, and $E\,^1\Pi(0) \rightarrow X\,^1\Sigma^+(0)$ resonance transitions were measured. In addition, excitation functions $[B\,^1\Sigma^+(0) \rightarrow X\,^1\Sigma^+(0)$ and $C\,^1\Sigma^+(0) \rightarrow X\,^1\Sigma^+(0)]$ and oscillator strengths have been determined, using a modified-Born-approximation analytic fit to the measured excitation function.

PACS number(s): 34.80.Gs

INTRODUCTION

Carbon monoxide is the most abundant interstellar molecule after H_2 and its isotopic variants [1] and is an important constituent in the atmosphere of Venus [2]. Theoretical descriptions of the abundance, excitation, and destruction mechanisms of CO are limited due to the lack of quantitative spectroscopic data for CO in the vacuum ultraviolet spectral region [3]. A better understanding of the destruction mechanism of CO is necessary for studies of airglow emission from planetary atmospheres, as well as for studies of comets and for models of the chemistry of the interstellar medium [2]. Photochemical models of interstellar clouds have been described in detail by numerous investigators [4–8]. The main destruction mechanism for CO in the interstellar regions is considered to be photodissociation. The abundance of CO relative to H_2 in the interstellar region has not been well understood theoretically. The rate at which the CO molecule is photodissociated by uv starlight is one of the major theoretical uncertainties [1]. This rate governs the C-to-CO ratio, the abundance of CO, and its growth with depth in diffuse interstellar clouds and the outer parts of thick molecular clouds [1]. Reviews of photodissociation processes of astrophysical molecules which emphasize the need for improved data for CO were compiled by van Dishoeck [9,10]. Most recently Morton and Noreau [11] have compiled wave numbers, wavelengths, and oscillator strengths for about 1500 electronic transitions in the CO molecule and compared the compiled data with existing uv observations.

Photodissociation of CO occurs in the wavelength range $91.2 < \lambda < 111.8$ nm [1]. Numerous experimental studies of the electronic states of CO lying above the dissociation limit have been performed in recent years [3,12–24]. Photodissociation of a molecule can take place either directly by continuous absorption into the repulsive part of an excited electronic state or indirectly by discrete line absorption into predissociating states [9].

Laboratory experiments have revealed no significant continuous absorption into the repulsive part of an excited electronic state at wavelengths greater than 91.2 nm [3,14,15,17]. Quantum-mechanical calculations of the electronic structure of CO by Cooper and Kirby [25] supported this conclusion. It was therefore concluded that the dissociation of CO must take place predominantly through predissociation of bound states and not directly through continuum states [1]. In order to fully understand the abundance, excitation, and dissociation mechanisms of CO in the interstellar medium, high-resolution spectroscopic studies of CO in the energy range 10.7–13.6 eV are required.

In this paper, we report, as a continuation of our previous work [20], the electron-impact-induced emission spectra of CO corresponding to the extreme ultraviolet (euv) transitions from the $B\,^1\Sigma^+$, $C\,^1\Sigma^+$, and $E\,^1\Pi$ states to the $X\,^1\Sigma^+$ ground state for 20-, 100-, and 200-eV electron-impact energies. In order to separate the many blended spectral bands, the present measurements were carried out at 20 times higher spectral resolution [0.025 nm full width at half maximum (FWHM)] than our previous measurements. Emission cross sections corresponding to the $B\,^1\Sigma^+(0) \rightarrow X\,^1\Sigma^+(0)$, $C\,^1\Sigma^+(0)$ $\rightarrow X\,^1\Sigma^+(0)$, and $E\,^1\Pi(0) \rightarrow X\,^1\Sigma^+(0)$ transitions were measured. In addition, excitation functions (0–1 keV) extending well into the Born region have been measured for the resonance transitions $[B\,^1\Sigma^+(0) \rightarrow X\,^1\Sigma^+(0)$, and $C\,^1\Sigma^+(0) \rightarrow X\,^1\Sigma^+(0)]$ allowing the oscillator strengths to be determined using a modified Born approximation analytic fit to the shape of the measured excitation function [26,27].

EXPERIMENTAL APPARATUS

The experimental apparatus, calibration procedure, and cross-section measurement technique have been described in our recent publications [28,29]. In brief, the medium-resolution 1.0-m spectrometer system was used

51   2067

in the present measurements. It consists of an electron-impact collision chamber in tandem with an uv spectrometer. The spectrometer has a resolution capability of 0.025 nm on repeated and single spectral scans, verified by scanning the Ar 104.8-nm resonance line. With equal entrance and exit slits the instrument response function was triangular. uv emission spectra of CO were measured by crossing a magnetically collimated beam of electrons with a beam of CO gas formed by a capillary array. Emitted photons, corresponding to radiative decay of collisionally excited states of CO, were detected by the uv spectrometer equipped with a chaneltron detector. The resulting emission spectra, measured at 20-, 100-, and 200-eV incident electron beam energies were calibrated for relative sensitivity as a function of wavelength according to the procedures described by Ajello et al. [30]. In order to determine the absolute value of the emission cross section corresponding to each measured feature, one additional procedure (normalization) must be applied. The absolute cross section of the spectral feature at 83.38 nm, at 200-eV electron-impact energy, was chosen to normalize the relative intensities of the transitions from the $B\,^1\Sigma^+(0)$, $C\,^1\Sigma^+(0)$, and $E\,^1\Pi(0)$ vibronic states of CO. The O II (83.38 nm) fluorescence signal produced by dissociative ionization of CO at 200-eV impact energy was compared with the fluorescence signal from the CO $C\,^1\Sigma^+(0) \rightarrow X\,^1\Sigma^+(0)$ emission band at 108.79 nm at 200-eV impact energy under the identical gun conditions. A background gas pressure of about 1×10^{-5} Torr was used to avoid self-absorption effects on the $C\,^1\Sigma^+(0,0)$ band, as discussed below. A well-established absolute emission cross-section value of $(1.80\pm0.39)\times10^{-19}$ cm^2 for O II (83.38 nm) [20], at 200 eV, was used to normalize the signal strength of the CO $C\,^1\Sigma^+(0,0)$ band, at 200 eV, to an absolute emission cross-section value of $(58.9\pm14.7)\times10^{-19}$ cm^2.

The background gas pressure for the present determination of CO emission cross sections was carefully chosen to ensure optically thin conditions and to avoid self-absorption effects, particularly for the $C\,^1\Sigma^+(0,0)$ band at 108.79 nm. The operating pressure must result in an optical depth at line center of less than 0.1 for the optical path involved. Below this pressure the measured cross section will be independent of pressure. The following approach has been used to determine the maximum background gas pressure that can be used and still maintain optically thin conditions. The relative intensities of the $C\,^1\Sigma^+(0,0)$ band at 108.79 nm and the O II g $^4S^o\cdot ^4P$ multiplet at 83.38 nm have been measured as a function of pressure over the range $8\times10^{-8} - 8\times10^{-4}$ Torr. The symbol g is used to denote the ground term. The O II line is not expected to exhibit any optical depth effects in this pressure range and acts as a normalization feature. The intensity ratio of these features is shown in Fig. 1 and is approximately constant up to a background gas pressure of 2×10^{-5} Torr when it begins to decrease, indicating the onset of self-absorption at 108.79 nm.

No corrections for polarization of the radiation were made. Polarization of the radiation is considered to be small where many rotational lines contribute to a vibrational band for an excited molecule.
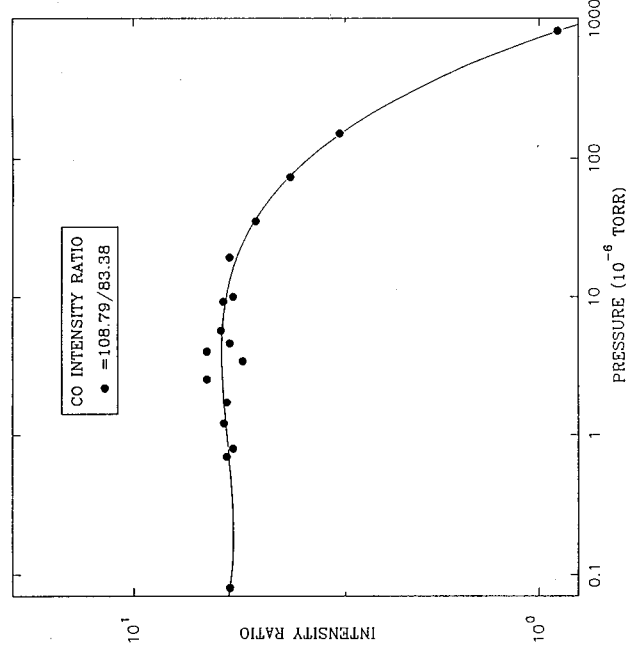

FIG. 1. The intensity ratio of the CO $C\,^1\Sigma^+(0,0)$ band at 108.79 nm and the CO O II $g\,^4S^o\cdot ^4P$ multiplet at 83.38 nm as a function of CO background gas pressure. The ratio is approximately constant up to about 2.0×10^{-5} Torr and starts decreasing, indicating the onset of self-absorption of the CO $C\,^1\Sigma^+(0,0)$ band at 108.79 nm. The O II $g\,^4S^o\cdot ^4P$ at 83.38-nm multiplet signal, which exhibits no optical depth effects, acts as a normalization feature.

EXPERIMENTAL RESULTS AND DISCUSSION

Medium-resolution, electron-impact emission spectra of CO in the euv region, at 20, 100, and 200 eV, are shown in Figs. 2, 3, and 4, respectively. These spectra were obtained under optically thin conditions, at a spectral resolution of 0.025 nm (FWHM), and calibrated for wavelength. The background gas pressure was 1×10^{-5} Torr. The spectral features are identified in the figures. The spectral region from 107.4 to 109.2 nm includes the direct euv transitions from the $E\,^1\Pi(0)$ and $C\,^1\Sigma^+(0)$ excited vibronic states of CO. At the present resolution, the observed $E\,^1\Pi(0)$ and $C\,^1\Sigma^+(0)$ features correspond exclusively to molecular transitions in CO. The spectral region from 114.8 to 115.4 nm contains the euv transition from the $B\,^1\Sigma^+(0)$ excited state of CO, which is blended with an atomic component (O I $^1D\cdot ^1D^o$ at 115.2 nm) at 100- and 200-eV electron-impact energies (Figs. 3 and 4). At 20 eV, an energy below the threshold for dissociative excitation of atomic multiplets, the $B\,^1\Sigma^+$ feature corresponds purely to molecular transitions in CO. Table I lists the candidate identifications of each feature observed at this spectral resolution together with the measured absolute emission cross sections at 20-, 100-, and 200-eV electron-impact energies. The root-sum-square uncertainty in the absolute cross sections given in this work was estimated to be 25% based on the uncertainties in the O II (83.3-nm) cross section, relative calibration, and signal statistics [28].
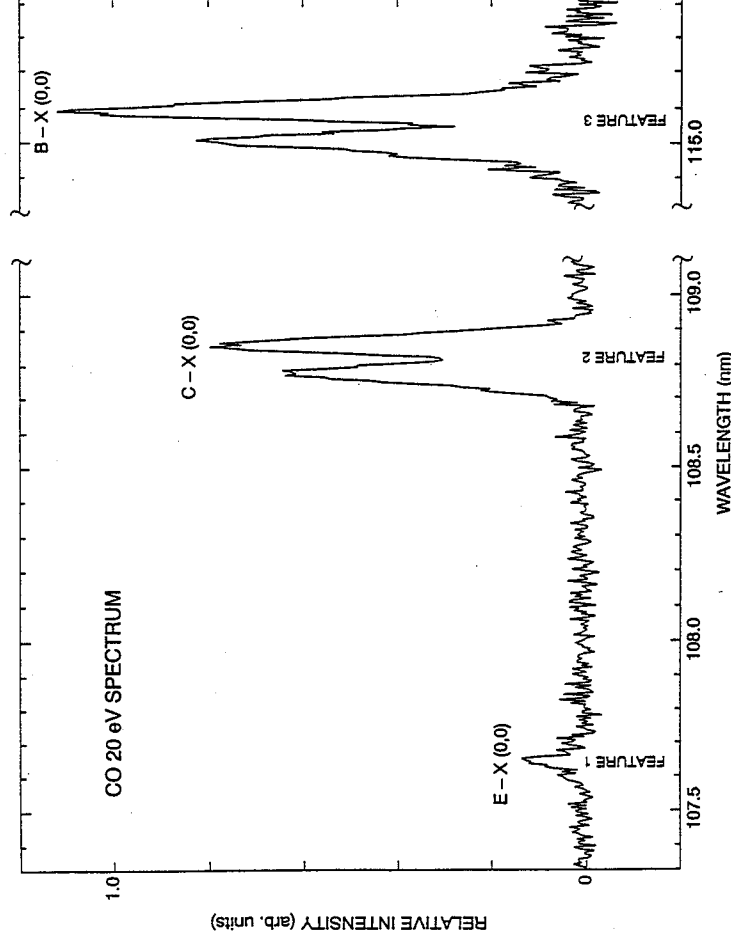
The strongest feature observed in the 100- and 200-eV

FIG. 2. Calibrated, medium-resolution (0.025 nm FWHM) electron-impact spectrum of CO at 20 eV. The spectrum was obtained in the crossed-beam mode at 1.0×10^{-5} Torr background gas pressure. P and R branches are separated for the C-$X(0,0)$ and B-$X(0,0)$ transitions. Emission cross sections for the identified features are listed in Table I.

emission spectra of CO corresponds to the $C\,^1\Sigma^+$ → $X\,^1\Sigma^+(0,0)$ resonance band. This feature contains approximately 98% of the observed euv emission between the $C\,^1\Sigma^+$ state and the $X\,^1\Sigma^+$ state [20]. This is supported by consideration of unperturbed Rydberg-Klein-Rees (RKR) Franck-Condon factors calculated for the C→X system. Letzelter et al. reported the branching ratio loss to be 7% via the C→A emission channel [17]. Excitation functions measured in the ranges 0–250 eV

and 0–1.0 keV are shown in Figs. 5 and 6, respectively. The excitation function shapes are typical of a dipole-allowed transition. The excitation function for CO $C\,^1\Sigma^+$ →$X\,^1\Sigma^+(0,0)$ resonance band at 108.79 nm, from 0 to 250 eV (Fig. 5), was used to determine the 200–20-eV and 200–100-eV emission cross section ratios. These ratios were needed to obtain the absolute emission cross sections for the CO $C\,^1\Sigma^+(0)$→$X\,^1\Sigma^+(0)$ band at 20- and 100-eV electron-impact energies at 0.025 nm (FWHM)
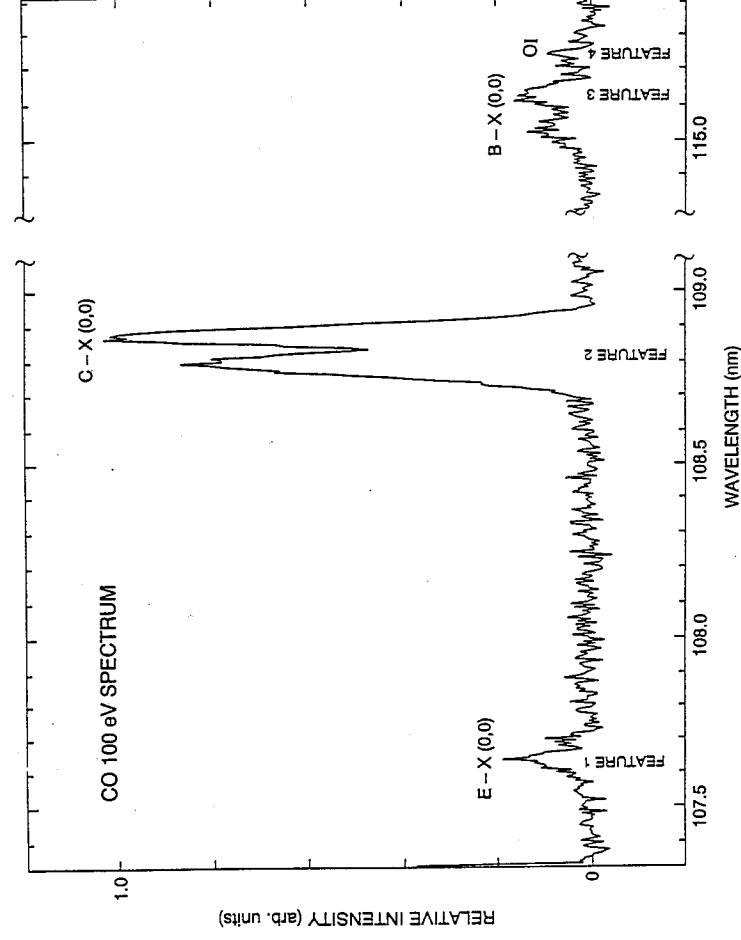

FIG. 3. Calibrated, medium-resolution (0.025 nm FWHM) electron-impact spectrum of CO at 100 eV. The spectrum was obtained in the crossed-beam mode at 1.0×10^{-5} Torr background gas pressure. P and R branches are separated for the C-$X(0,0)$ and B-$X(0,0)$ transitions. Emission cross sections for the identified features are listed in Table I.
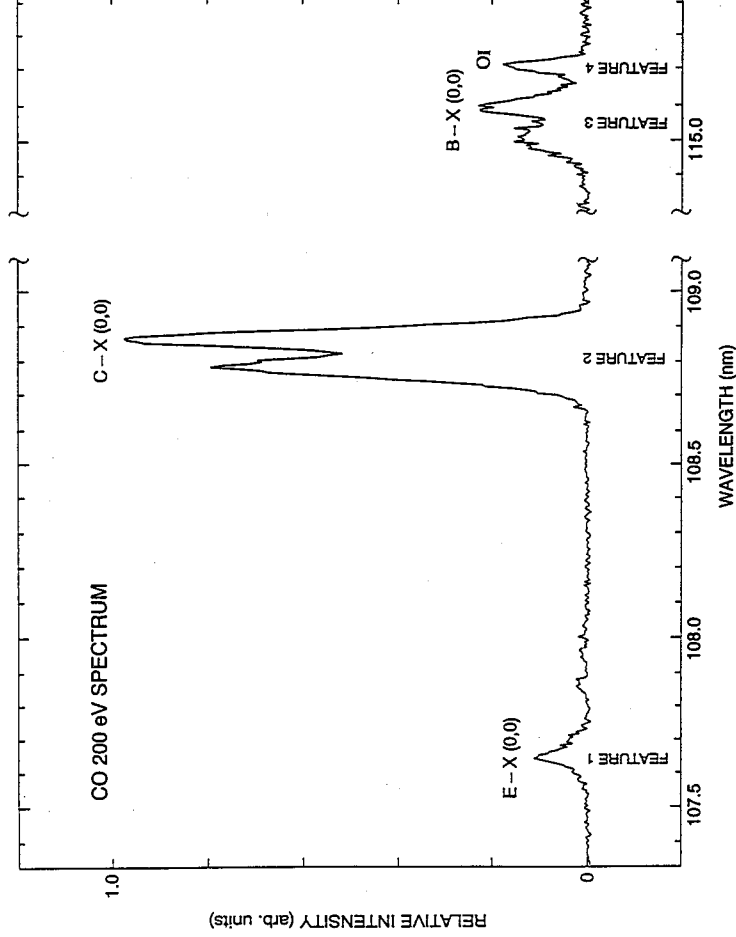
FIG. 4. Calibrated, medium-resolution (0.025 nm FWHM) electron-impact spectrum of CO at 200 eV. The spectrum was obtained in the crossed-beam mode at 1.0×10^{-5} Torr background gas pressure. P and R branches are separated for the C-$X(0,0)$ and B-$X(0,0)$ transitions. Emission cross sections for the identified features are listed in Table I.

spectral resolution.

The strongest feature observed in our 20-eV spectrum is the $B\,^1\Sigma^+ \to X\,^1\Sigma^+(0,0)$ band. Based on our previous paper [20], the $B\,^1\Sigma^+ \to X\,^1\Sigma^+(0,0)$ band represents 96% of the observed euv emission from the B state of CO. The B state decays only by two radiative channels: through $B \to X$ transitions in the uv and through $B \to A$ transitions in the visible spectral region. Letzelter et al. reported the fluorescence yield of the $B \to A$ transition (i.e., branching ratio loss) as 40% [17]. As shown in Fig. 7, $B\,^1\Sigma^+ \to X\,^1\Sigma^+(0,0)$ band exhibits a striking anomaly in the energy dependence of its emission cross section. In our earlier publication [20], we argued that this may be attributed either to an electron exchange process or to a near threshold resonance of the O I multiplet, which blended with the $B\,^1\Sigma^+(0,0)$ feature. The higher-resolution (0.025-nm) excitation function measurement of the $B\,^1\Sigma^+(0)$ vibronic state indicated that spin exchange plays a large part in the excitation of the $v'=0$ level of the $B\,^1\Sigma^+$ state (since the O I multiplet was resolved and excluded from this measurement). This is also supported by differential cross-section measurements for the electron-impact excitation of the $B\,^1\Sigma^+$ state at 20 eV [23]. Those measurements showed no strong for-

ward peaking, but fairly isotropic angular distribution. It should be pointed out that even though the B state is designated as a singlet state, the very sharp peak in the excitation function of the $B\,^1\Sigma^+(0)$ state (Fig. 7), at low electron-impact energies, should arise from spin exchange from a significant triplet admixture. The singlet character of this state dominates at higher energies in the excitation function.

The $E\,^1\Pi \to X\,^1\Sigma^+$ system was observed in our spectra by the appearance of the (0,0) resonance band. No excitation function measurement for the $E\,^1\Pi(0) \to X\,^1\Sigma^+(0)$ transition was made since the emission from this band is found to be very weak. No other transitions of the $E \to X$ system were observed. RKR Franck-Condon factor calculations, on the other hand, indicate that about 95% of the euv emission from this state to the ground state occurs via the (0,0) transition [20].

Oscillator strengths

Previous experimental and theoretical determinations of oscillator strengths $f_{v'v''}$ from $v''=0$ of the $X\,^1\Sigma^+$ ground state of CO to different v' levels of the $B\,^1\Sigma^+$ and $C\,^1\Sigma^+$ states have been summarized by Kirby and Coop-

TABLE I. Vibronic emission cross sections of CO at 20, 100, and 200 eV.

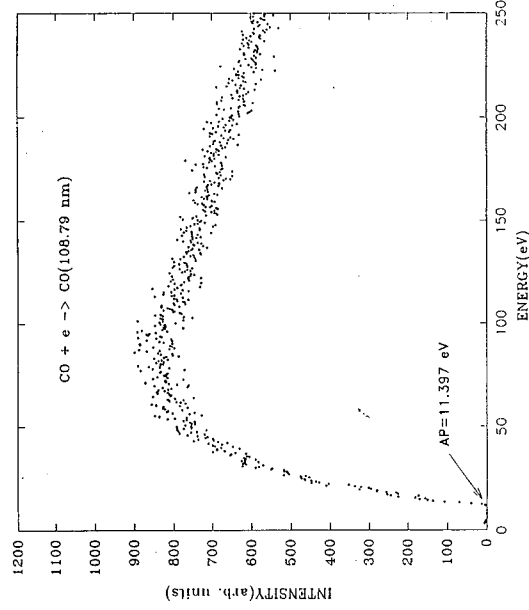| Feature No.	Species	Wavelength (nm)	Term	Vibronic emission cross section (10^{-18} cm^2)		
				20 eV	100 eV	200 eV
1	CO	107.61	$3p\pi E\,^1\Pi(0)-X\,^1\Sigma^+(0)$	0.21	0.47	0.39
2	CO	108.79	$C\,^1\Sigma^+(0)-X\,^1\Sigma^+(0)$	2.58	7.40	5.89
3	CO	115.05	$B\,^1\Sigma^+(0)-X\,^1\Sigma^+(0)$	3.48	1.88	1.42
4	O I	115.21	$^1D-{}^1D^o$		0.35	0.37

FIG. 5. Relative emission cross section (excitation function) of the CO $C^1\Sigma^+(0,0)$ band at 108.79 nm from 0- to 250-eV electron-impact energy. The appearance potential (AP) shown in the figure is at 11.397 eV.
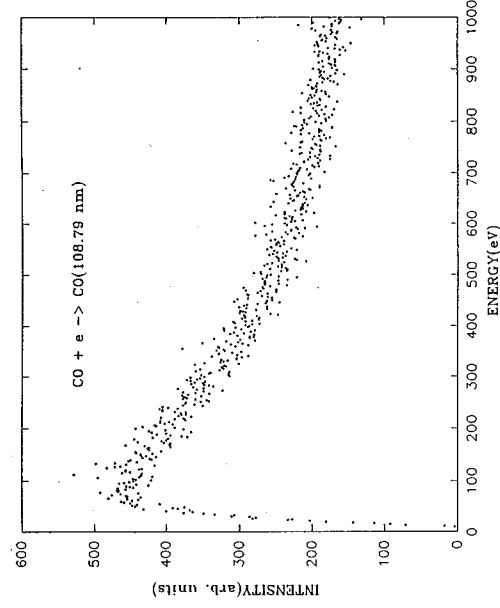

FIG. 6. Relative emission cross section (excitation function) of the CO $C^1\Sigma^+(0,0)$ band at 108.79 nm from 0- to 1000-eV electron-impact energy.
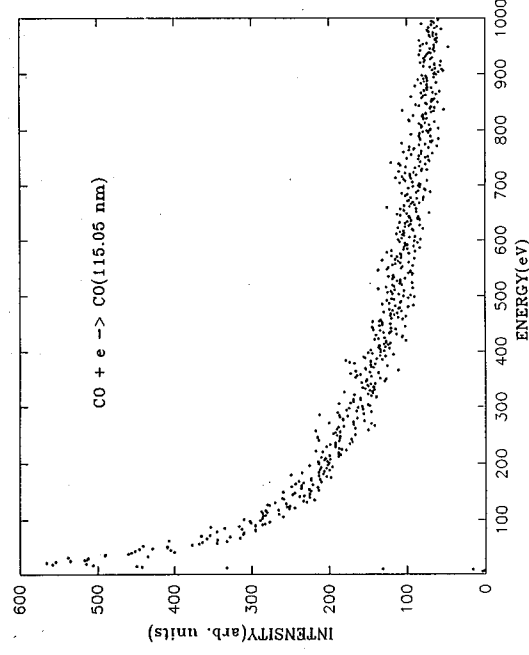

FIG. 7. Relative emission cross section (excitation function) of the CO $B^1\Sigma^+(0,0)$ band at 115.05 nm from 0- to 1000-eV electron-impact energy.

er [2]. This summary has been updated to include the work of Chan, Cooper, and Brion [22] and is shown together with present results in Table II.

We obtain the oscillator strengths for the $C^1\Sigma^+(v'=0)\rightarrow X^1\Sigma^+(v''=0)$ and $B^1\Sigma^+(v'=0)\rightarrow X^1\Sigma^+(v''=0)$ transitions by analyzing the energy dependence of the measured excitation functions (from 0 to 1 keV) corresponding to those transitions. The excitation functions for the $C^1\Sigma^+(v'=0)\rightarrow X^1\Sigma^+(v''=0)$ and $B^1\Sigma^+(v'=0)\rightarrow X^1\Sigma^+(v''=0)$ transitions (Figs. 6 and 7, respectively) are put on an absolute scale by normalizing them to the present measurements of 200-eV

emission cross sections for the $C^1\Sigma^+(v'=0)\rightarrow X^1\Sigma^+(v''=0)$ and $B^1\Sigma^+(v'=0)\rightarrow X^1\Sigma^+(v''=0)$ transitions, respectively. The emission cross sections for the B-$X(0,0)$ and C-$X(0,0)$ vibronic transitions, given in Table I, were corrected for the branching ratio losses to a lower excited state ($A^1\Pi$) based on the data of Letzelter et al. [17]. The correction is 40% for the B-$X(0,0)$ transition and 7% for the C-$X(0,0)$ transition. Cascade contributions from the $E^1\Pi$ state to the B-$X(0,0)$ and C-$X(0,0)$ band systems are negligible [20].

Collision strength data (cross section times electron impact energy) for the resonance bands of CO ($C^1\Sigma^+$ and $B^1\Sigma^+$) were fitted using the following analytical form for collision strength:

$$\Omega_{v'v''}(X_{v'v''}) = C_0(1-1/X_{v'v''})(X_{v'v''}^{-2})$$
$$+\sum_{k=1}^{4} C_k(X_{v'v''}-1)\exp(-kC_8X_{v'v''})$$
$$+C_5+C_6/X_{v'v''}+C_7\ln(X_{v'v''}), \qquad (1)$$

where $\Omega_{v'v''}(X_{v'v''})$ is the collision strength, $X_{v'v''}$ is the electron-impact energy in threshold units, and C_k are constants of the function $\Omega_{v'v''}(X_{v'v''})$ [26,27]. The constant C_0 represents the contribution of electron exchange, C_1-C_4 represent configuration mixing, C_5-C_6 represent polarization effects, C_7 is the Born term, and C_8 is a constant in the mixing terms. Table III gives the constants of Eq. (1) for the CO $B^1\Sigma^+(v'=0)\rightarrow X^1\Sigma^+(v''=0)$ and $C^1\Sigma^+(v'=0)\rightarrow X^1\Sigma^+(v''=0)$ transitions. The excitation cross section is given by the equation

$$\sigma_{v'v''}(X_{v'v''}) = \Omega_{v'v''}(X_{v'v''})(E_{v'v''}X_{v'v''})^{-1}, \qquad (2)$$

where $\sigma_{v'v''}(X_{v'v''})$ is the cross section in atomic units and

ISIK KANIK, GEOFFREY K. JAMES, AND JOSEPH M. AJELLO

TABLE II. Summary of previous determinations of oscillator strengths $f_{v'v''}$ ($\times 10^{-2}$) for the transitions between the different v' levels of the CO $B\,^1\Sigma^+$ and $C\,^1\Sigma^+$ states and the ground state $X\,^1\Sigma^+(v''=0)$.

Source	v'	0	1	2	3
		$B\,^1\Sigma^+$			
Aarts and de Heer [12]		1.5			
Lassettre and Skerbele [13]		1.53±0.14			
Lee and Guest [15]		0.24±0.04			
Letzelter et al. [17]		0.45	0.07	3.7×10^{-3}	
Kirby and Copper [2] (theory)		0.21	0.03	6×10^{-4}	
Chan, Cooper, and Brion [22]		0.803	0.132		
Present		1.15±0.3			
		$C\,^1\Sigma^+$			
Aarts and de Heer [12]		16.0			
Lassettre and Skerbele [13]		16.3±1.5			
Lee and Guest [15]		1.27±0.19			
Letzelter et al. [17]		6.19	0.28	$<1\times10^{-3}$	4.4×10^{-3}
Kirby and Copper [2] (theory)		11.81	0.18	4×10^{-4}	1×10^{-6}
Chan, Cooper, and Brion [22]		11.77	0.356		
Present		15.4±4.1			

$E_{v'v''}$ is the transition energy in Rydberg units. At the high-energy limit the collision strength has the form

$$\Omega_{v'v''}(X_{v'v''})\approx C_5+C_7\ln(X_{v'v''})\,,\quad X_{v'v''}\gg 1\,. \qquad (3)$$

In the Bethe approximation [27,31], the collision strength is given by

$$\Omega_{v'v''}(X_{v'v''})=\omega_{v'}\left[\frac{8ma_0^2}{\hbar^2}\right]\left[\frac{f_{v'v''}}{E_{v'v''}}\right](\ln X_{v'v''}+4C_{v'v''}E_{v'v''})\,, \qquad (4)$$

where $\omega_{v''}$ is the lower state degeneracy, $C_{v'v''}$ is a constant related to the angular distribution of the scattered electrons, $f_{v'v''}$ is the oscillator strength, a_0 is the Bohr radius, m is electron mass, and $\hbar$ is Planck's constant. A comparison of Eqs. (3) and (4) gives us C_7, one of the constants in the fitting function, which can be related to the optical oscillator strength at the high-energy limit. That is,

$$C_7=\omega_{v''}\left[\frac{8ma_0^2}{\hbar^2}\right]\left[\frac{f_{v'v''}}{E_{v'v''}}\right]. \qquad (5)$$

As seen in Eq. (5), we can determine the optical oscillator strength. For the CO $C\,^1\Sigma^+(0)\rightarrow X\,^1\Sigma^+(0)$ and $B\,^1\Sigma^+(0)\rightarrow X\,^1\Sigma^+(0)$ transitions the optical oscillator strengths were found to be $(15.4\pm4.1)\times10^{-2}$ and $(1.15\pm0.30)\times10^{-2}$, respectively. The experimental excitation functions and fitting functions for the CO $C\,^1\Sigma^+(0)X\,^1\Sigma^+(0)$ and $B\,^1\Sigma^+(0)\rightarrow X\,^1\Sigma^+(0)$ transitions are shown in Figs. 8 and 9, respectively. The errors associated with the oscillator strengths are

TABLE III. Constants of the modified Born equation.
$\Omega_{ij}(X)=C_0(1-1/X)(X^{-2})+\sum_{k=1}^{4}C_k(X-1)\exp(-kC_8X)+C_5$
$+C_6/X+C_7\ln(X)$.

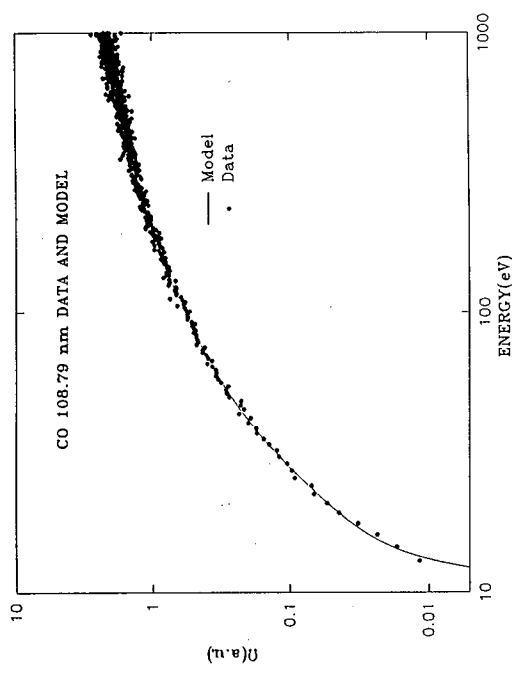| Constant	$B\,^1\Sigma^+$	$C\,^1\Sigma^+$
C_0	0.127 86	0.0
C_1	−0.088 66	0.361 30
C_2	0.189 46	−0.460 74
C_3	−0.309 05	2.625 40
C_4	0.0	0.0
C_5	0.235 18	−1.1700
C_6	−0.235 18	1.1700
C_7	0.058 363	0.738 11
C_8	0.158 49	0.602 56

FIG. 8. Model and data of the collision strength of the CO $C\,^1\Sigma^+(0,0)$ band at 108.79 nm plotted against energy (10–1000 eV). The oscillator strength (f value) for this feature is determined as 0.154.
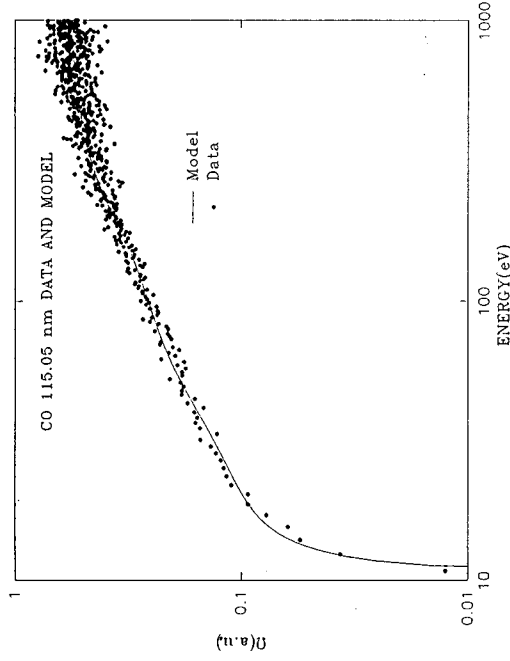
FIG. 9. Model and data of the collision strength of the CO $B^1\Sigma^+(0,0)$ band at 115.05 nm plotted against energy (10–1000 eV). The oscillator strength (f value) for this feature is determined as 1.15×10^{-2}.

estimated as follows: (a) 25% error from the cross-section measurements and (b) 5% error from the fitting procedure. In addition, it should be pointed out that the presence of the low-energy secondary electrons in the electron beam can alter the shape of an excitation function in the high-energy region and hence potentially result in an increase in the measured value of C_7 and hence the optical oscillator strength. Our measurements [32] showed that this effect could give us an additional error of up to 10% in the oscillator strength. Thus the overall error (square root of the sum of the squares of the contributing errors) in the oscillator strengths is estimated to be about 27%.

There are many reported experimental measurements of the oscillator strengths of the $B^1\Sigma^+$ and $C^1\Sigma^+$ states. Large variations have been found among these values. For the $B^1\Sigma^+(0)\rightarrow X^1\Sigma^+(0)$ transition, a comparison of the available oscillator strengths gives fair agreement between the present determination and those of Aarts and de Heer [12], Lassettre and Skerbele [13], and Chan, Cooper, and Brion [22]. The present result is about 30% lower than that of Aarts and de Heer [12] and 33% lower than that of Lassettre and Skerbele [13]. The present measurement is, however, about 30% larger than the most recent result of Chan, Cooper, and Brion [22]. The discrepancy between the present measurement and the results of other investigators [2,15,17] is found to be quite large. The other results are 2.5–5.5 times smaller than the present result.

For the $C^1\Sigma^+(0)\rightarrow X^1\Sigma^+(0)$ transition, a comparison of the oscillator strengths gives excellent agreement between the present result and those of Aarts and de Heer [12] (4% higher than ours) and Lassettre and Skerbele [13] (about 6% higher than ours). The theoretical result of Kirby and Cooper [2] is about 23% lower than ours. The value of Lee and Guest [15] is smaller than ours by an order of magnitude. Our value is about 2.5 times larger than the measurement of Letzelter et al. [17]. However, our study shows that the $C^1\Sigma^+$ resonance band is subject to pressure saturation effects. Since pressure effects increase with increasing oscillator strength, the effect of self-absorption of radiation in the C state will be much larger than for the B state. Therefore, the values of the oscillator strengths reported by Lee and Guest [15] and Letzelter et al. [17] for the $C^1\Sigma^+\rightarrow X^1\Sigma^+$ transition may well be affected by pressure saturation effects. The most recent result of Chan, Cooper, and Brion [22] is in fairly good agreement with the present result (the disagreement is about 23%).

SUMMARY AND CONCLUSION

We have measured the electron-impact-induced emission spectra of CO corresponding to the euv transitions of the $B^1\Sigma^+$, $C^1\Sigma^+$, and $E^1\Pi$ states to the $X^1\Sigma^+$ ground state for 20-, 100-, and 200-eV electron-impact energies. The present measurements were carried out at a spectral resolution of 0.025 nm (FWHM). Excitation function measurements from 0 to 1.0 keV for two resonance transitions [$C^1\Sigma^+(0)\rightarrow X^1\Sigma^+(0)$ and $B^1\Sigma^+(0)\rightarrow X^1\Sigma^+(0)$] were performed. The corresponding oscillator strengths were determined using a modified Born approximation analytic fit to the shape of the measured excitation function [26,27]. For the $B^1\Sigma^+(0)\rightarrow X^1\Sigma^+(0)$ transition, a comparison of the oscillator strengths gives fair agreement between the present finding and the results of Aarts and de Heer [12], Lassettre and Skerbele [13], and Chan, Cooper, and Brion [22]. The disagreement between the present and other results is, however, quite large, as seen in Table II. For the $C^1\Sigma^+\rightarrow X^1\Sigma^+$ process, a comparison of the oscillator strengths gives excellent agreement with the experimental values of Aarts and de Heer [12], and Lassettre and Skerbele [13]. The experimental value of Chan, Cooper, and Brion [22] and the theoretical value of Kirby and Cooper [2] are also in fairly good agreement with our result. Large discrepancies exist between the other reported sets and the present result.

Serious discrepancies exist among the limited measurements of cross sections and oscillator strengths reported for CO. There is a definite need for further measurements to improve on the present situation. Further investigations of this type, at room temperature and in a low-temperature regime, are needed. The importance of low-temperature measurements to learn more details about molecular clouds was pointed out by van Dishoeck and Black [5].

The scope of this paper is limited to the measurement of the emission cross sections and oscillator strengths of the direct euv transitions to the ground state. However, the importance of accurate determination of the predissociation rates for the excited states of CO was strongly emphasized by several investigators [1,3,19]. The predissociation rates for the low rotational levels of both the $E^1\Pi(0)\rightarrow X^1\Sigma^+(0)$ and $E^1\Pi(1)\rightarrow X^1\Sigma^+(0)$ bands are especially important to understand the isotope-selective photodissociation of CO [1]. The emission cross sections can be used to estimate the predissociation yields by com-

parison with the corresponding electron-impact excitation cross sections obtained from electron energy-loss measurements provided any cascading components to and from (i.e., branching loss) the states in question are taken into account. This type of approach, however, is not a very meaningful way to determine a small predissociation yield (typically 20% or smaller) of a state if the predissociation yield lies within the combined percent error limit (typically about 25%) for the emission and the excitation cross sections. Instead, a high-resolution study of the properties of CO rotational structure at a variety of temperatures (20–300 K), employing the perturbed thermal model [33] fit to the data, is a more meaningful and sensitive probe for weak predissociation. This approach has been used in our laboratory for the determination of predissociation yields of the

$c_4'\,^1\Sigma^+(0) \rightarrow X\,^1\Sigma^+(0)$ state of N_2 [32]. Laboratory measurements of high-spectral-resolution (up to 0.0015 nm), optically thin uv emission spectra of CO, at a variety of temperatures (20–300 K), are in progress to determine J-level-dependent predissociation rates.

[1] E. F. van Dishoeck and J. H. Black, Astrophys. J. **334**, 771 (1988).

[2] K. Kirby and D. L. Cooper, J. Chem. Phys. **90**, 4895 (1989).

[3] G. Stark, K. Yoshino, P. L. Smith, K. Ito, and W. H. Parkinson, Astrophys. J. **369**, 574 (1991).

[4] J. H. Black and A. Dalgarno, Astrophys. J. Suppl. **34**, 405 (1977).

[5] E. F. van Dishoeck and J. H. Black, Astrophys. J. Suppl. **62**, 109 (1986).

[6] E. F. van Dishoeck and J. H. Black, in *Physical Processes in Interstellar Clouds*, edited by G. E. Morfill and M. Scholer (Reidel, New York, 1987), p. 241.

[7] E. F. van Dishoeck and J. H. Black, in *Rate Coefficients in Astrochemistry*, edited by T. J. Millar and D. A. Williams (Kluwer Academic, Deventer, 1988), p. 209.

[8] E. F. van Dishoeck, in *Highlights of Astronomy*, edited by D. McNally (Reidel, Dordrecht, 1989), p. 323.

[9] E. F. van Dishoeck, in *Astrochemistry*, edited by M. S. Vardya and S. P. Tarafdar (Reidel, Dordrecht, 1987), p. 51.

[10] E. F. van Dishoeck, in *Rate Coefficients in Astrochemistry* (Ref. [7]), p. 49.

[11] D. C. Morton and L. Noreau (private communication).

[12] J. F. M. Aarts and F. J. de Heer, J. Chem. Phys. **52**, 5354 (1970).

[13] E. N. Lassettre and A. Skerbele, J. Chem. Phys. **54**, 1597 (1971).

[14] J.-H. Fock, P. Gurtler, and E. E. Koch, Chem. Phys. **47**, 87 (1980).

[15] L. C. Lee and J. A. Guest, J. Phys. B **14**, 3415 (1981).

[16] M. Eidelsberg, F. Launay, F. Rostas, A. Le Floch, J. Breton, and B. Thieblemont, Ann. Israel Phys. Soc. **6**, 240 (1984).

[17] C. Letzelter, M. Eidelsberg, F. Rostas, J. Breton, and B. Thieblemont, Chem. Phys. **114**, 273 (1987).

[18] K. Yoshino, G. Stark, P. L. Smith, W. H. Parkinson, and K. Ito, J. Phys. (Paris) Colloq. **49**, C1-37 (1988).

[19] M. Eidelsberg and F. Rostas, Astron. Astrophys. **235**, 472 (1990).

[20] G. K. James, J. M. Ajello, I. Kanik, B. Franklin, and D. E. Shemansky, J. Phys. B **25**, 1481 (1992).

[21] P. C. Cosby, J. Chem. Phys. **98**, 7804 (1993).

[22] W. F. Chan, G. Cooper, and C. E. Brion, Chem. Phys. **170**, 123 (1993).

[23] A. G. Middleton, M. J. Brunger, and P. J. O. Teubner, J. Phys. B **26**, 1743 (1993).

[24] I. Kanik, M. Ratliff, and S. Trajmar, Chem. Phys. Lett. **208**, 341 (1993).

[25] D. L. Cooper and K. Kirby, J. Chem. Phys. **87**, 424 (1987).

[26] D E. Shemansky, J. M. Ajello, and D. T. Hall, Astrophys. J. **296**, 765 (1985).

[27] D. E. Shemansky, J. M. Ajello, D. T. Hall, and B. Franklin, Astrophys. J. **296**, 774 (1985).

[28] J. M. Ajello, G. K. James, B. O. Franklin, and D. E. Shemansky, Phys. Rev. A **40**, 3524 (1989).

[29] G. K. James, J. M. Ajello, B. O. Franklin, and D. E. Shemansky, J. Phys. B **23**, 2055 (1990).

[30] J. M. Ajello, D. E. Shemansky, B. Franklin, J. Watkins, S. Srivastava, G. K. James, W. T. Simms, C. W. Hord, W. Pryor, W. McClintock, V. Argabright, and D. Hall, Appl. Opt. **27**, 890 (1988).

[31] H. A. Bethe, Ann. Phys. (N.Y.) **5**, 325 (1930).

[32] D. E. Shemansky, J. M. Ajello, and I. Kanik, J. Geophys. Res. (to be published).

[33] D. E. Shemansky, I. Kanik, and J. Ajello, J. Geophys. Res. (to be published).